



TEM study of helium bubble evolution in erbium ditritide

Gillian Bond¹,
Jim Browning² and Clark S. Snow²

¹New Mexico Institute of Mining and Technology

²Sandia National Laboratories

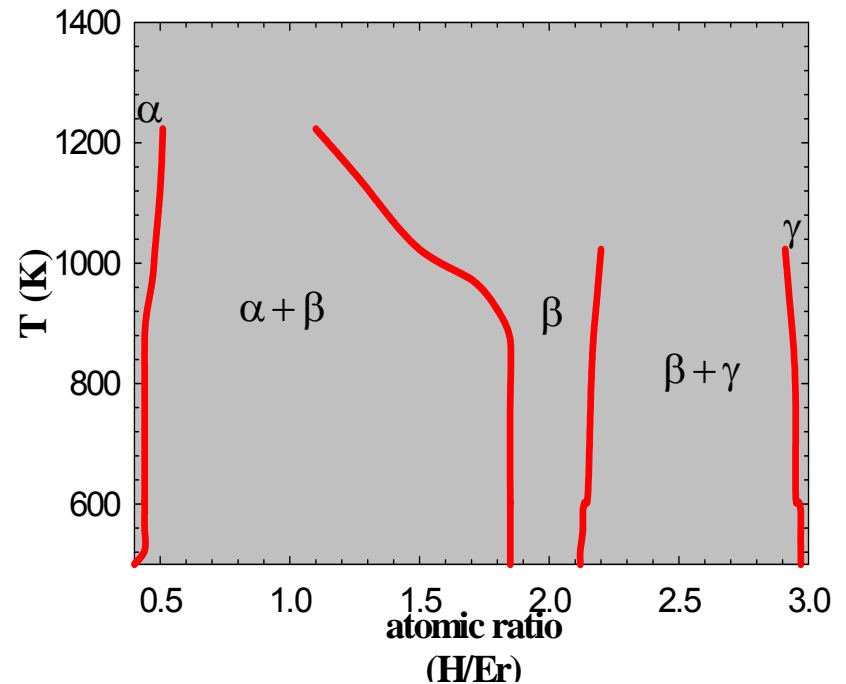
Hydrogen and Helium Isotopes in Materials Conference
February 6, 2007, Albuquerque, NM

Neutron generators

- Neutron generators are small electrostatic accelerators that:
 - exploit the d-D and d-T nuclear reactions for the production of 2.5 and 14.1 MeV neutrons, respectively
 - target and source materials are usually metal hydride systems
 - have applications in medical and geological research and energy exploration, as well as defense and security applications

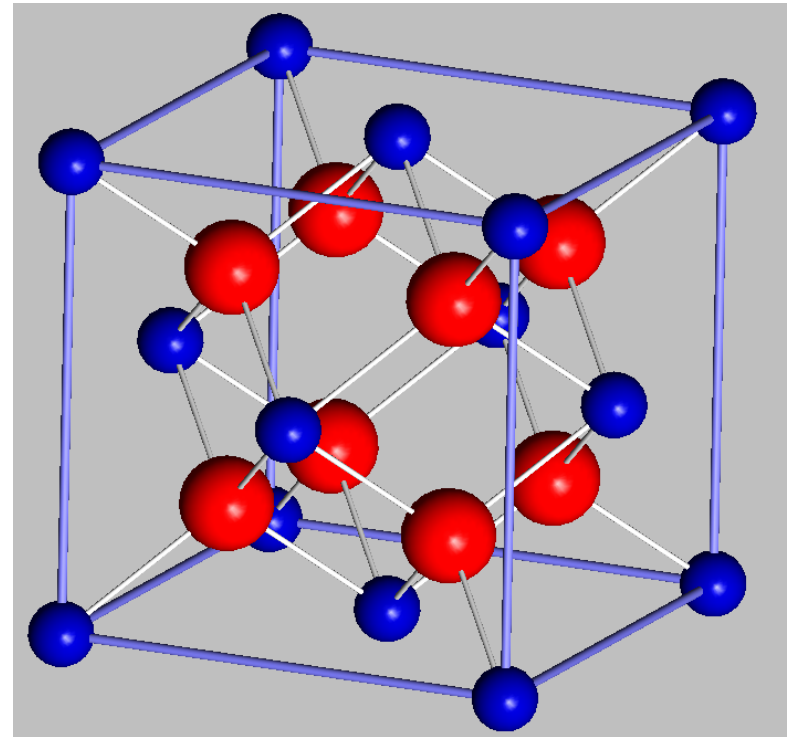
Rare-earth hydrides

- Rare-earth hydrides possess the ability to accommodate hydrogen concentrations up to three times the atomic concentration of the host metal.
- Erbium hydrides are used in neutron generators.



Crystal structure

- The dihydride, or β -phase, assumes the CaF_2 structure with hydrogen atoms (nominally) occupying tetrahedral sites.



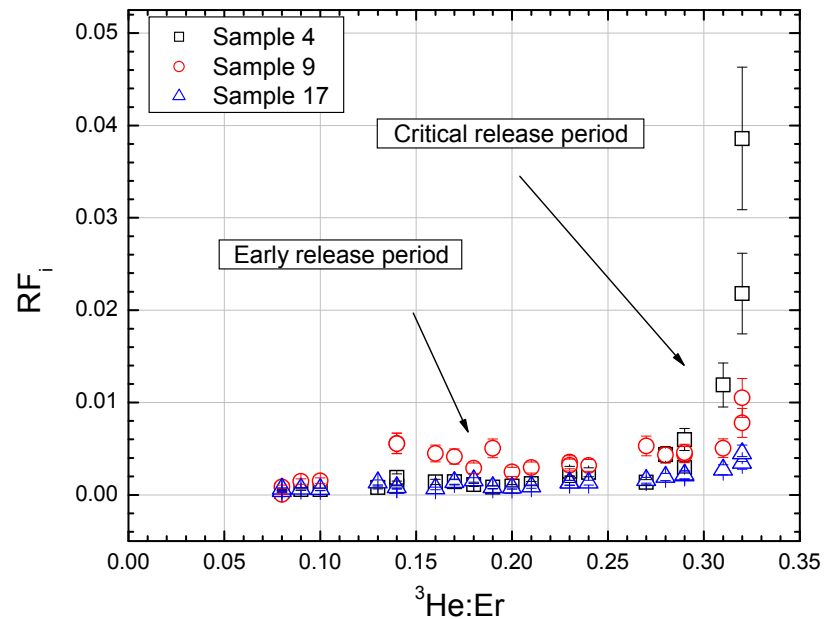
Helium generation in tritides

- Tritium, the radioactive isotope of hydrogen, is required for the production of 14 MeV neutrons
 - Transmutation of tritium to helium-3 is an issue to be considered when selecting a metal hydride for use in neutron generator technology
 - ^3He has time-dependent effects on the structure and properties of the host metal hydride
 - ^3He emission from the host metal hydride is non-uniform and material dependent

Fundamentals of Helium Release from Metal Tritides



- Very small fraction of helium evolves from film.
- Release is characterized by two phases
 - Early release
 - Critical release



Samples

- (100) Si wafer as substrate
- 1000 Å Mo
- 5000 Å Er
- Sample preparation: Loren Espada (SNL)
- Er loading with T: Tom Venhaus (LANL)
- $\text{ErT}_2 \rightarrow \text{ErT}_{2-x}(\text{}^3\text{He}_x)$ with time
- Samples stored in vacuum

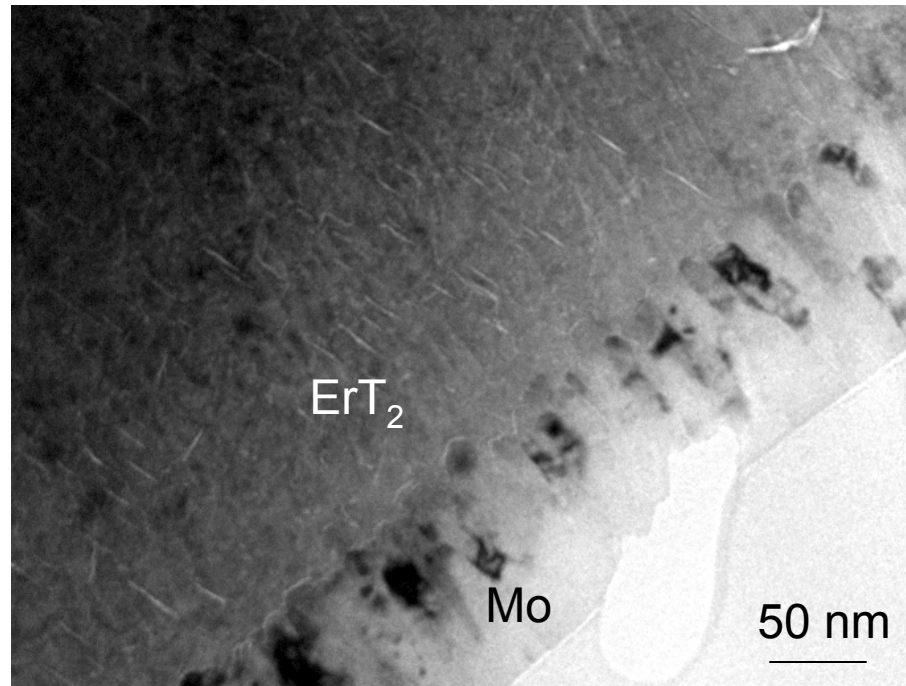
Sample characterization

- Ion Beam Analysis (IBA)
 - Er and initial T areal densities
 - ^3He concentration as a function of time is calculated from initial T concentration by application of well-known decay constant
- Transmission electron microscopy (TEM)
 - Both cross-sectional (CS) and plan-view (PV) samples
 - Sample preparation: Garry Bryant (SNL)

Cross-sectional TEM samples

- Wafer with films cleaved into strips
- Strips mounted in sandwich configuration
- Cross-section cut, ground and polished
- Sample dimpled until film thickness $\sim 10 \mu\text{m}$
- Ion milled at $\sim 3.5 - 4^\circ$ and 5kV until perforation
- Examined in JEOL JEM-2000FX TEM at 200 kV

ErT₂ /Mo films (540 days, He:Er 0.153)



- Smaller grain size of Mo
- Waviness of Er/Mo interface
- Cavitation at interface with particle of another phase

Helium release from near-surface region (Snow *et al.*)

- Studies on release from films of different thicknesses
- No demonstrable dependence of early helium release on film thickness
- Bubble-free “denuded” zone present at surface
- Suggest helium evolution is from surface region, while helium at greater depths is trapped in bubbles (at least during early release)

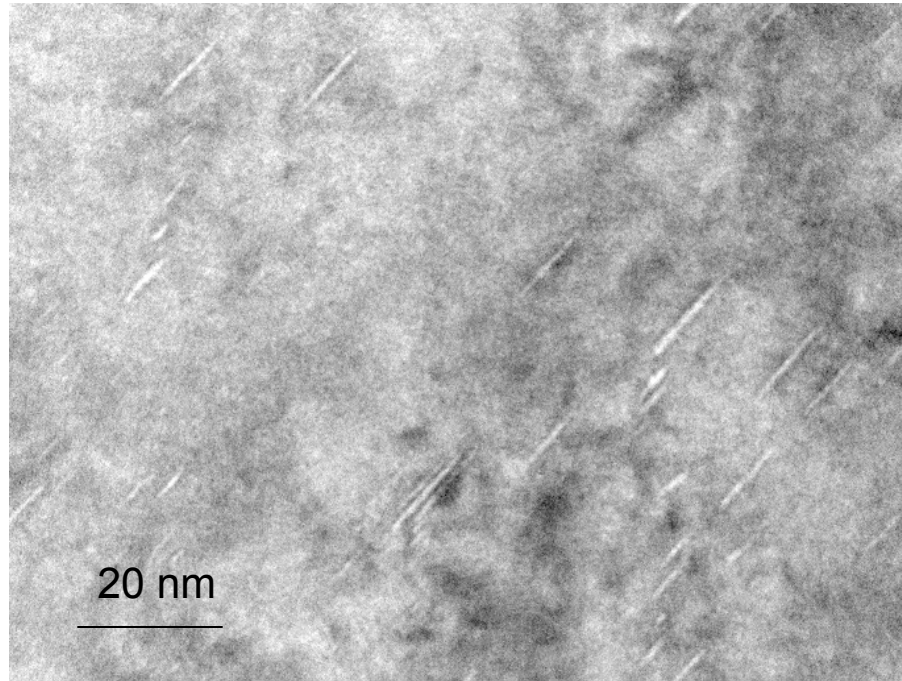
Development of helium bubbles: clustering and loop punching (Trinkaas)

- High He production rate and/or low T
- Clustering of helium atoms
- Cluster with $\sim 5-7$ helium atoms generates Frenkel pair
- Bubble growth proceeds by dislocation loop punching each time bubble pressure reaches $(2\gamma + \mu b)/r$
- Loop radius (r_l) assumed equal to bubble radius (r)
- γ treated as isotropic

Development of helium bubbles from nanocracks in e.g. ErT_2 (Cowgill)

- Plate-like bubble growth attributed to low surface energy favoring platelet growth by dipole expansion over bubble growth by dislocation loop punching
- He atoms cluster between $\{111\}$ planes to form nano-cracks
- First dipole formation occurs when nano-crack width is twice the interplanar spacing (at ~ 17 nm assuming same bubble density as in PdT_x)
- Surface energy of ErT_2 set at 0.637 GPa-nm

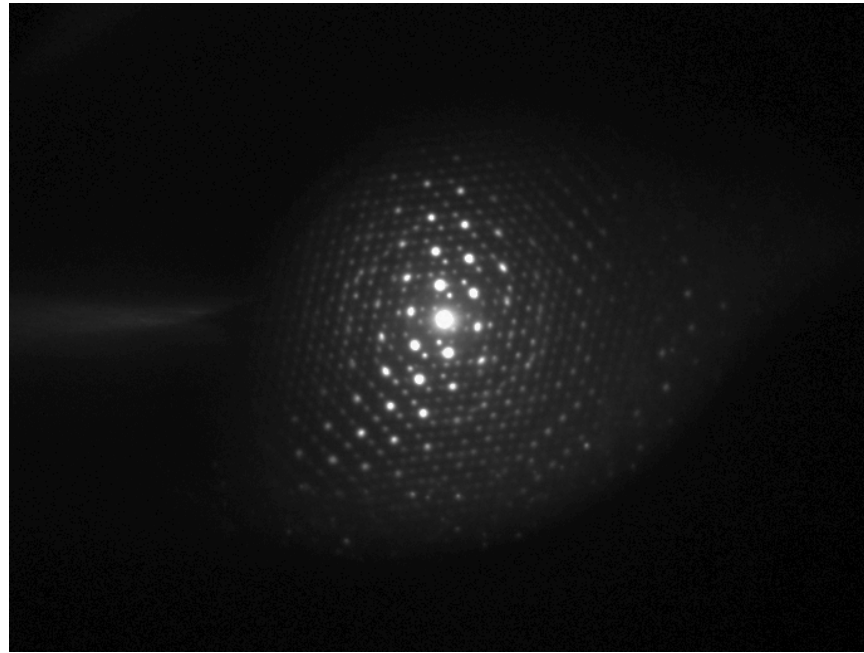
Helium bubbles 62 days after tritium loading, He:Er 0.018



Bright-field image, close to $\langle 110 \rangle$ zone axis,
cross section (CS)

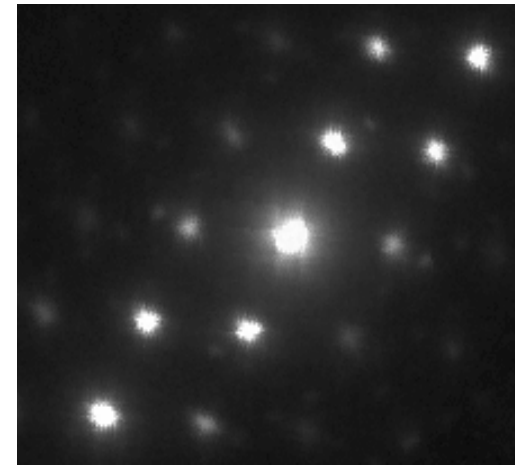
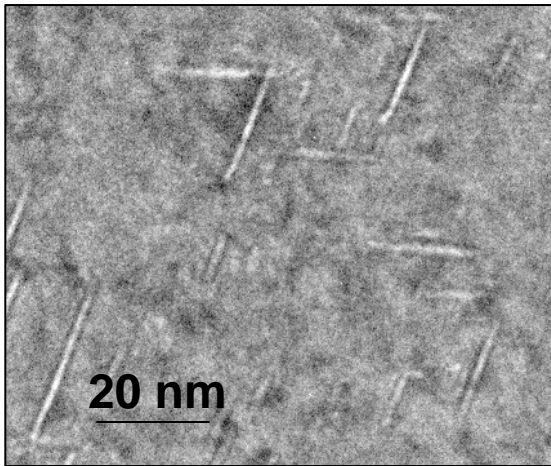
Additional diffraction spots

(He:Er 0.018)



- Observed in all our samples
- Observed also by Gelles, Kotula and Brewer
 - identified with small oxide precipitates ($\sim 5\text{nm}$)

Helium bubbles on {111} planes

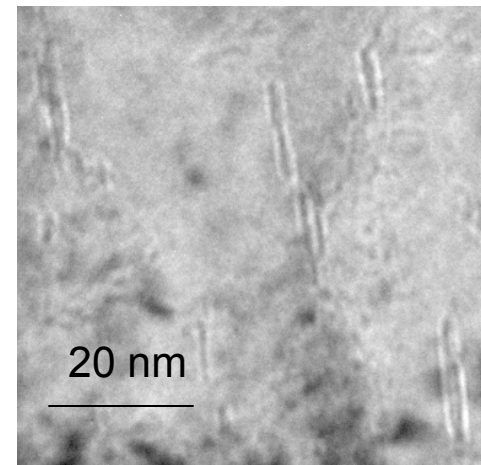
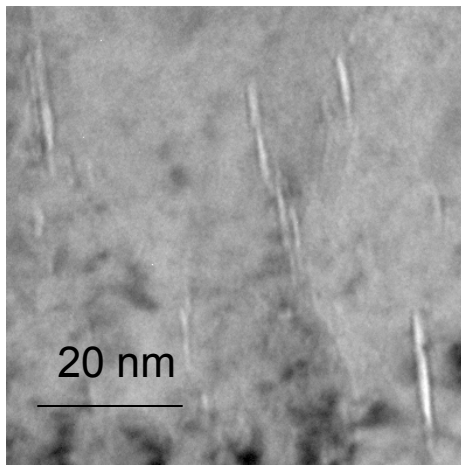
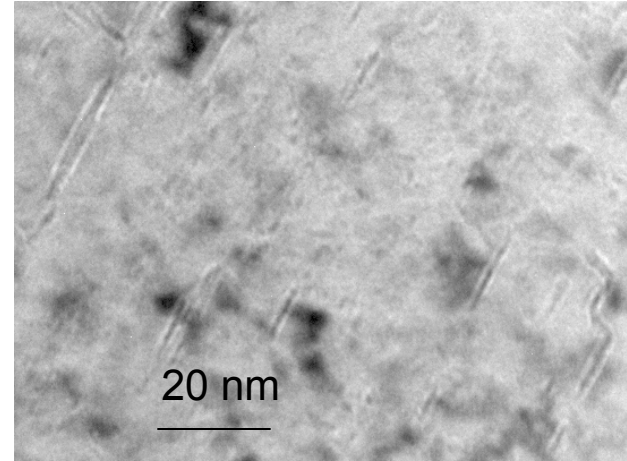
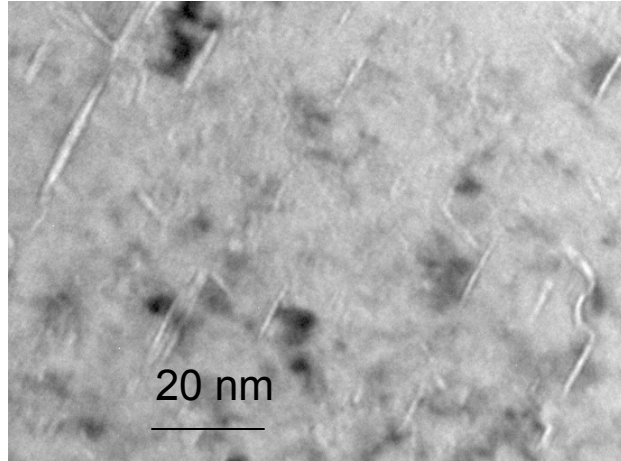


- a) Bright-field transmission electron micrograph
- b) Selected-area diffraction pattern close to $\langle 110 \rangle$ zone axis

Two sets of plate-like helium bubbles (at angle of $\sim 72^\circ$)

(206 days, CS, He:Er 0.060)

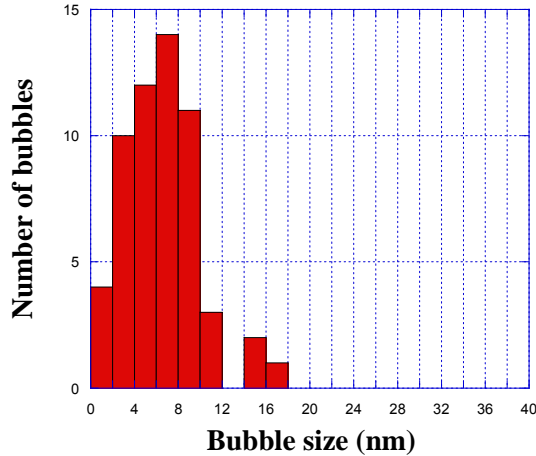
342 days, He:Er 0.098, plan view (PV), bright field, under and over focus



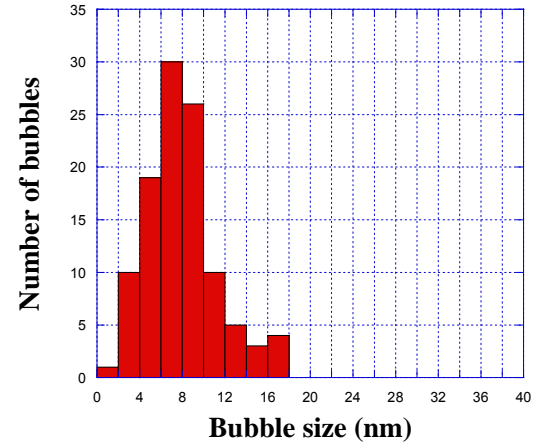
Histograms of bubble sizes

He:Er 0.018 – 0.060

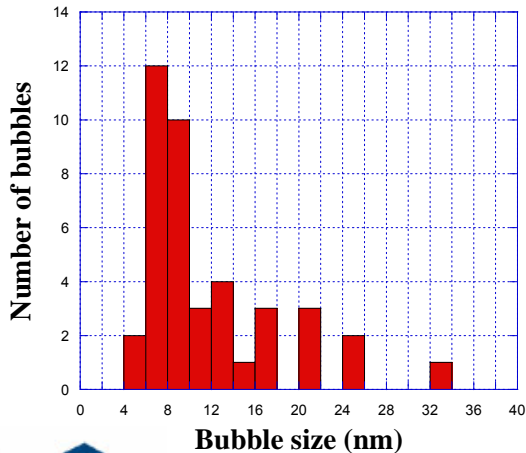
He:Er 0.018, CS, (n=57)



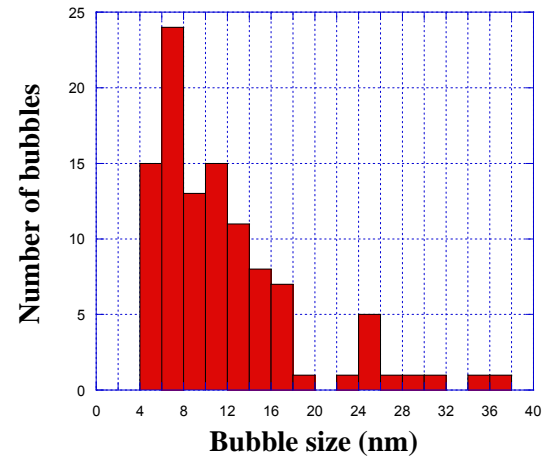
He:Er 0.031, CS, (n=108)



He:Er 0.055, CS, (n=190)



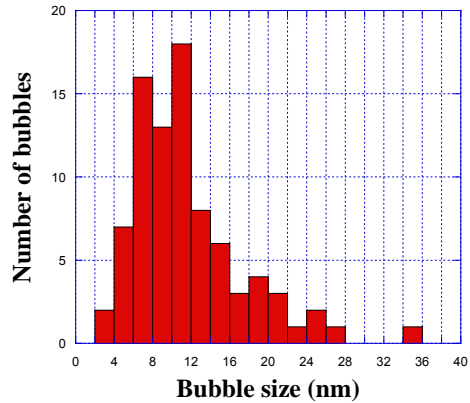
He:Er 0.06, CS, (n=105)



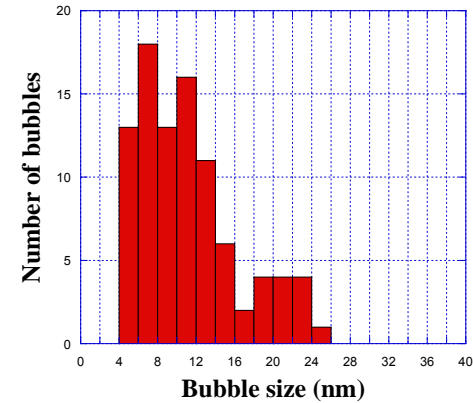
Histograms of bubble sizes

He:Er 0.066 – 0.074

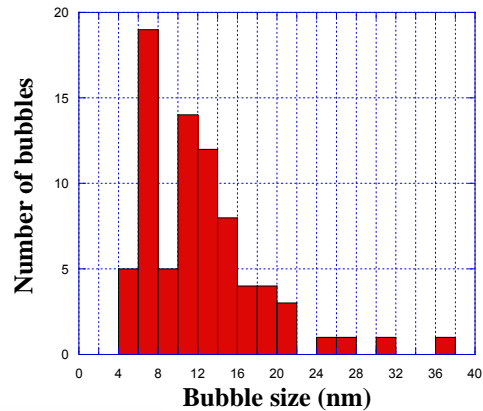
He:Er 0.066, CS
(n=85)



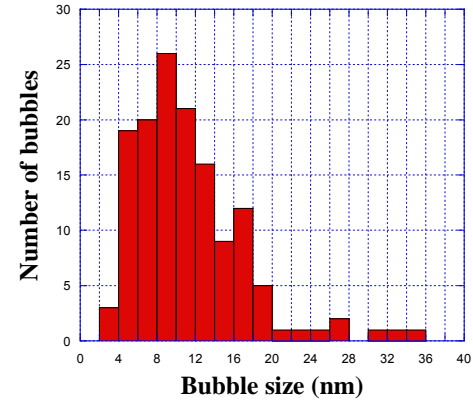
He:Er 0.066, PV
(n=92)



He:Er 0.070, CS
(n=78)



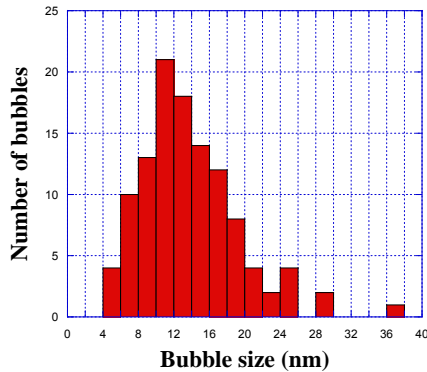
He:Er 0.074, PV
(n=139)



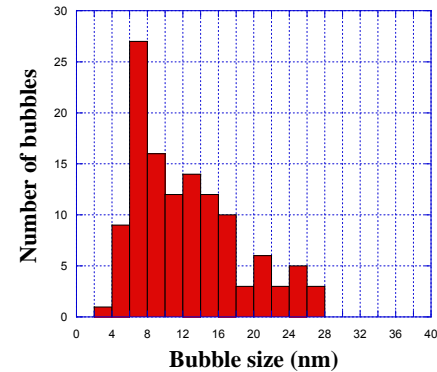
Histograms of bubble sizes

He:Er 0.079 – 0.108

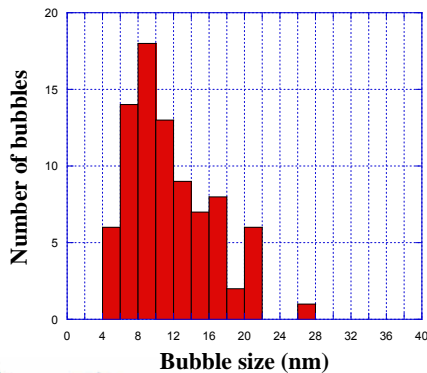
He:Er 0.079, CS
(n=113)



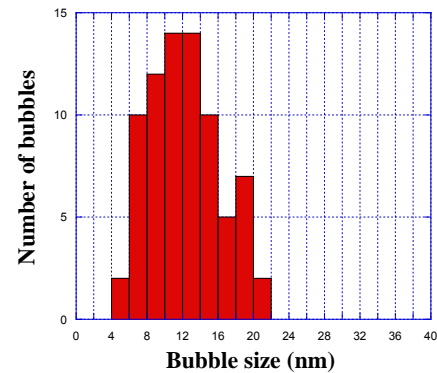
He:Er 0.079, PV
(n=121)



He:Er 0.098, PV
(n=84)

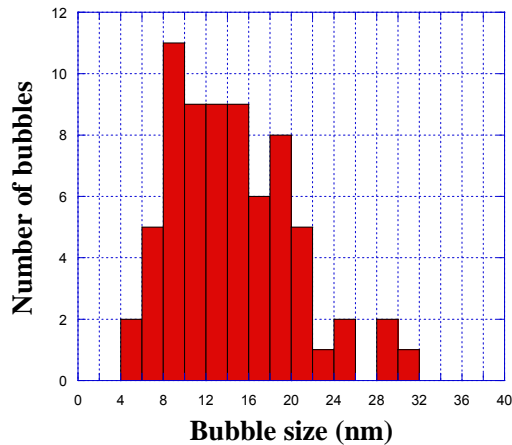


He:Er 0.108, CS
(n=76)

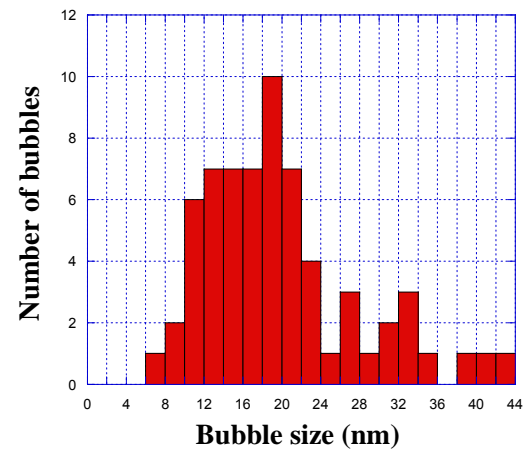


Histograms of bubble sizes: He:Er 0.112 – 0.143 compared to 0.018

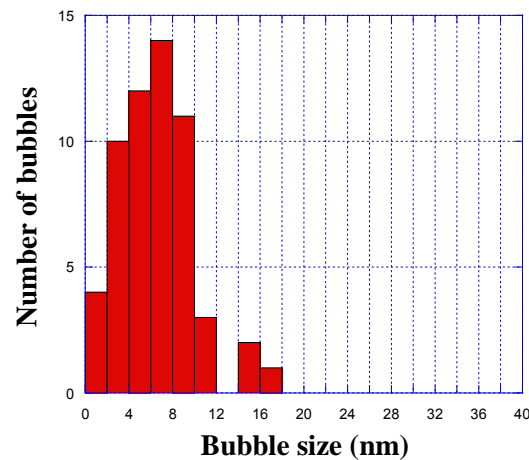
He:Er 0.112, CS
(n=70)



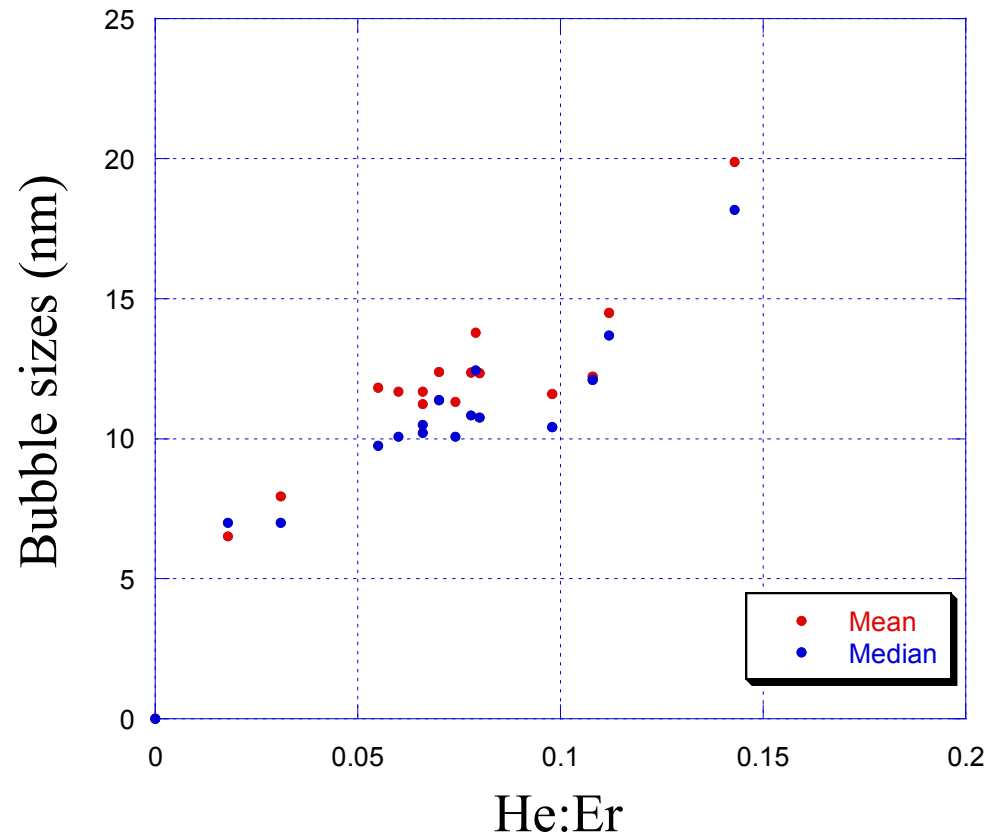
He:Er 0.143, PV
(n=65)



He:Er 0.018, CS
(n=57)

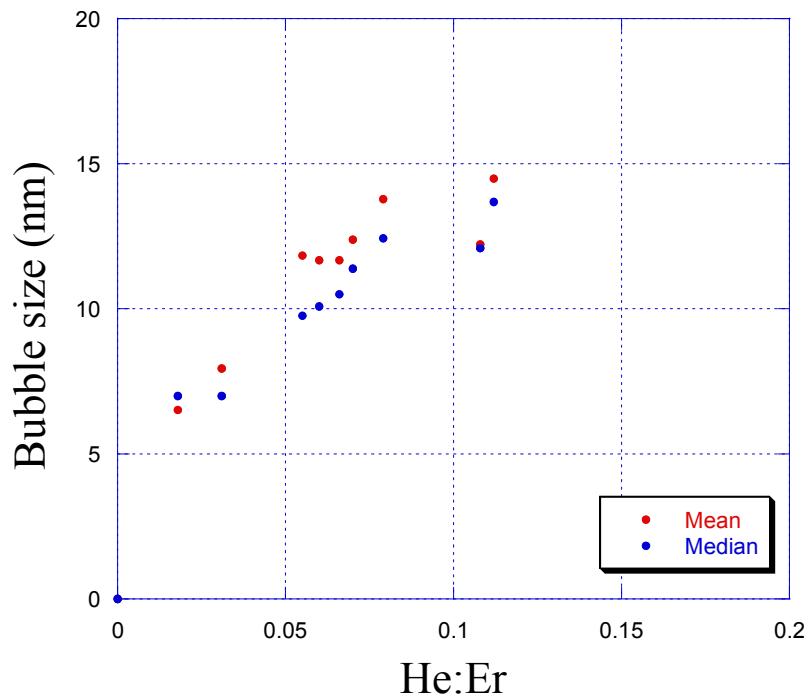


Mean and median bubble sizes

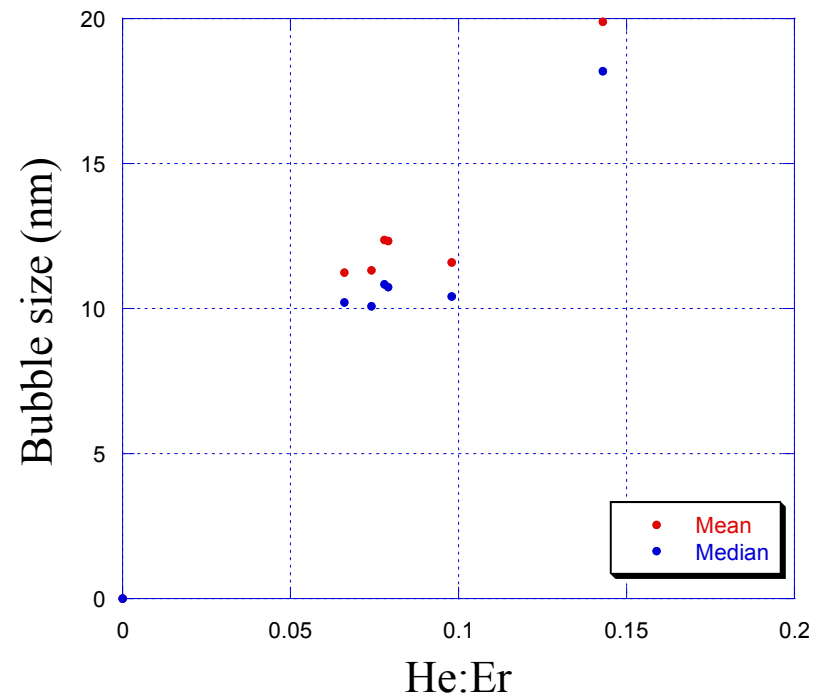


Mean and median bubble sizes: CS and PV

CS

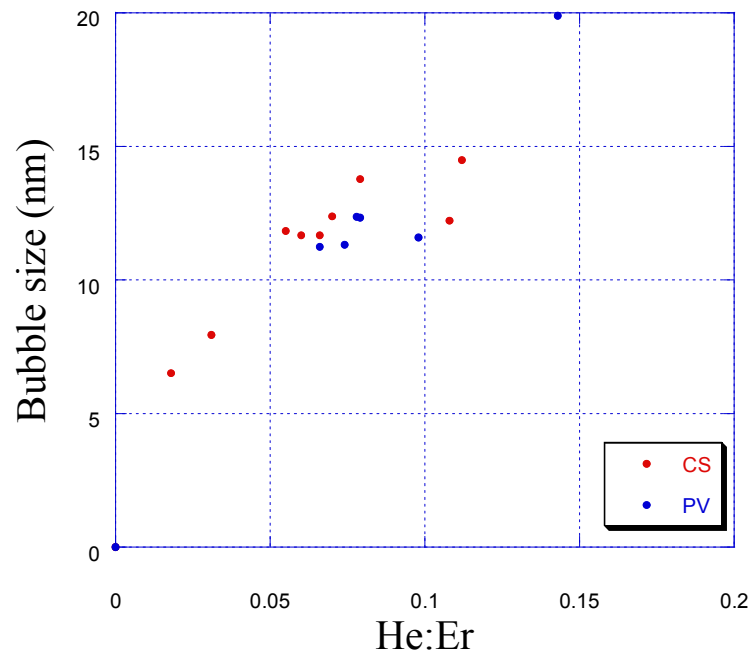


PV

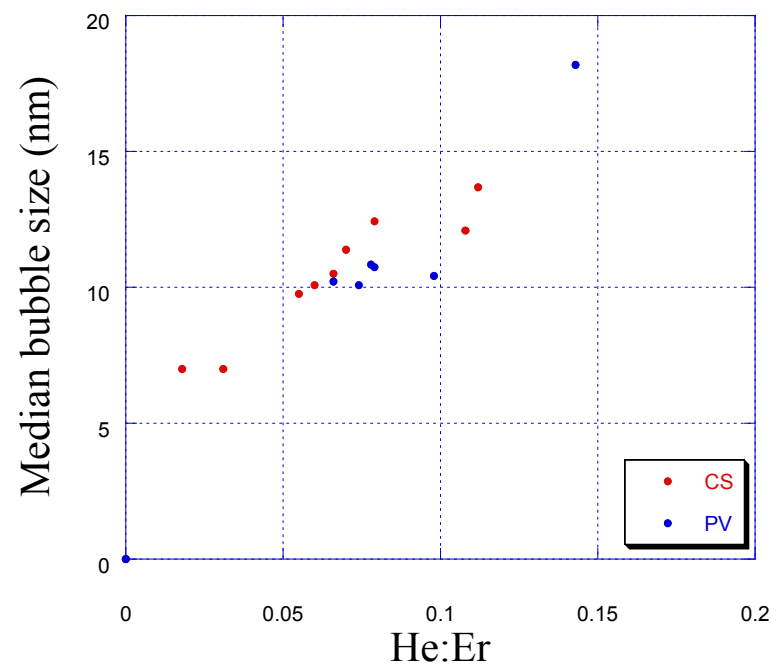


Mean and median bubble sizes

Mean bubble sizes: CS and PV



Median bubble sizes: CS and PV



Development of helium bubbles

- Nucleation appears to be completed early in bubble development
- Thickness of bubbles (platelets) observed by TEM is sometimes variable along a bubble
- Steps, consistent with “terrace and step” migration of an interface, are seen at smaller bubble sizes than ~ 17 nm
- Observations do not support punching of loops with $r_i = r$
- Cracks are seen to develop from bubbles, and to connect bubbles
- Presence of oxide particles in material

Interfacial energies

- Helium occupies octahedral sites in ErT_2
- Helium has very low solubility in ErT_2
- We need to consider here the ErT_2/He interfacial energy
- Density functional theory predicts strong tendency for T to segregate to $\{111\}$ faces of He bubbles (Jennison)
- This implies a large dependence of interfacial energy on crystallographic orientation

Questions

- Appropriate values and anisotropy of γ ?
- Effect of γ anisotropy on interface migration?
- Effect of H adsorption on interface migration?
- Adsorption/ γ effects as contributors to reason for loops/dipoles smaller than r ?
- Effects of oxides and/or solute O on He clustering and bubble nucleation?
- Effects of oxides and/or solute O on energy required for formation of Er self-interstitials or loops or dipoles?

Questions

- Effects of hydrogen on cracking and bubble linkage?
- Concentration of hydrogen in hydrostatic stress field ahead of nanocracks?
- Dependence of behavior on stoichiometry?
- Effect of bubble thickness (crack blunting)?
- Effects of local stress and strain fields?
- Effects of local defect structure?
- Influence of vacancy concentrations?

Acknowledgment

- Sandia is a multiprogram laboratory operated by Sandia Corporation, a Lockheed Martin Company, for the United States Department of Energy under contract DE-AC04-94AL85000.